

# Intra-unit-cell Magnetic Order in Stoichiometric $\text{La}_2\text{CuO}_4$

Vyacheslav G. Storchak,<sup>1,\*</sup> Jess H. Brewer,<sup>2</sup> Dmitry G. Eshchenko,<sup>3</sup> Patrick W. Mengyan,<sup>4</sup>  
Oleg E. Parfenov,<sup>1</sup> Andrey M. Tokmachev,<sup>1</sup> Pinder Dosanjh,<sup>2</sup> and Sergey N. Barilo<sup>5</sup>

<sup>1</sup>*National Research Centre “Kurchatov Institute”, Kurchatov Sq. 1, Moscow 123182, Russia*

<sup>2</sup>*Department of Physics and Astronomy, University of British Columbia, Vancouver, BC, Canada V6T 1Z1*

<sup>3</sup>*Bruker BioSpin AG, Industriestrasse 26, 8117 Fällanden, Switzerland*

<sup>4</sup>*Department of Physics, Texas Tech University, Lubbock, Texas 79409-1051, USA*

<sup>5</sup>*Institute of Solid State and Semiconductor Physics, Minsk 220072, Belarus*

(Dated: 1 May 2014)

Muon spin rotation measurements supported by magnetization experiments have been carried out in a stoichiometric high- $T_c$  parent compound  $\text{La}_2\text{CuO}_4$  in a temperature range from 2 K to 340 K and in transverse magnetic fields up to 5 T. Along with the antiferromagnetic local field, muon spin rotation spectra indicate presence of an additional source of magnetic field on the muon. The characteristic splitting of about 45 G coming from this additional magnetic field is consistent with spontaneous circulating currents model of Varma.

PACS numbers: 74.72.Cj, 75.45.+j, 75.50.Ee, 76.75.+i

The idea of a pseudogap (PG) has recently played a key role in our understanding of strongly correlated electron systems — particularly those exhibiting high- $T_c$  superconductivity (SC). Although some basic phenomenology of high- $T_c$  copper oxide superconductors — electron pairs with nonzero angular momentum, an exchange mechanism arising from strong Coulomb interaction between the valence electrons, and a remarkable departure from the standard Fermi liquid behavior in the normal state — is a matter of growing consensus, the microscopic mechanism still remains unclear. Understanding the origin of the PG and its relation to high- $T_c$  SC is considered an important step towards revealing this mechanism [1–3].

All of these cuprates, being hole (p) doped, have the same T-p phase diagram: at zero doping they are antiferromagnetic (AFM) Mott insulators while doping easily destroys the AFM and makes the system metallic. In the overdoped regime, the normal state exhibits properties of a correlated Fermi liquid. By contrast, in the underdoped regime of the phase diagram, cuprates show features of a correlated metal exhibiting non-Fermi-liquid behavior. Their transport, magnetic and thermodynamic properties point towards strong reduction of the electronic density of states (DOS) below a temperature  $T^*$ , although the DOS does not reach zero at the lowest temperature and the system remains metallic [1] — hence the PG terminology. Angle-resolved photoemission spectroscopy (ARPES) [4] suggests opening of a real gap in the one-particle excitation spectrum, supported by other spectroscopic techniques [3].

As doping dependence of the SC gap follows  $T^*$  rather than  $T_c$ , the PG has been considered as a precursor to the SC gap; the PG phase being a *disordered* state with broken phase coherence among preformed pairs, which condense below  $T_c$  as soon as phase coherence is established [5]. A different approach is presented by certain

models which consider the PG state as an *ordered* phase with a well defined order parameter and a related broken symmetry [6–8]. In this scenario,  $T^*$  is the transition temperature to an ordered PG phase of orbital magnetic moments caused by spontaneous circulating currents (CC). The fluctuations associated with the broken symmetry are considered to be responsible for both the superconductivity, playing role of a pairing glue, and the non-Fermi-liquid behavior below  $T^*$ .

To date, ARPES data are rather controversial: an apparent spontaneous dichroism of ARPES spectra of  $\text{Bi}_2\text{Sr}_2\text{CaCu}_2\text{O}_{8+\delta}$  [4] indicates a time-reversal symmetry breaking (TRSB) magnetic field in the PG phase — a fingerprint of an ordered state. Such dichroism, however, was not found in a later experiment [9]. The key experimental evidence for a novel ordered state comes from spin-polarized neutron scattering experiments, which report commensurate magnetic peaks below  $T^*$  in YBCO and Hg1201 [10–12], pointing to TRSB that, nevertheless, preserves lattice translation invariance, as the nuclear and magnetic peaks in reciprocal space are superimposed on Bragg reflections. Sizeable magnetic moments (on the order of 0.1–0.2  $\mu_B$ ) are reported in the PG state.

Positive muons, as local microscopic magnetic probes, are especially sensitive to any kind of magnetic order, manifested as a coherent muon spin oscillation with frequency proportional to the local magnetic field at the muon [13]. However, muon spin rotation ( $\mu\text{SR}$ ) experiments, which have convincingly demonstrated their sensitivity to TRSB fields in a number of weak magnetic systems, produced no evidence of magnetic order in the PG state. At first, spontaneous static magnetic fields were reported in YBCO [14], which were later reinterpreted as being due to spatial charge inhomogeneities [15]. No TRSB is reported in  $\text{La}_{2-x}\text{Sr}_x\text{CuO}_4$  (for  $x=0.13$  and  $x=0.19$ , both within the PG regime) where  $\mu\text{SR}$  ex-

periments set an upper limit of  $\sim 0.2$  G for any magnetic field at the muon site, while the expected TRSB local field is estimated to amount about 40 G [16]. This discrepancy between neutron and muon experiments has been attributed to screening of the charge density in the metallic-plane unit cells in the vicinity of the muon [17].

On the other hand, orbital currents and associated magnetic moments may well be present in the limiting case of the underdoped regime — insulating stoichiometric  $\text{La}_2\text{CuO}_4$  — should CC be an intimate feature of chemical bonding in the  $\text{CuO}_2$  plane. Recent studies of the phase diagram for high- $T_c$  cuprate SC suggest that CC loops do persist down to zero doping [18].

In this Letter, we present  $\mu\text{SR}$  spectroscopy of stoichiometric  $\text{La}_2\text{CuO}_4$ , in which the magnetic field at the muon should not be affected by charge density screening. Our data indicate *an additional source of magnetic field* at the muon site (over and above the previously known AFM field) consistent with Varma's model of circulating currents [6, 7] and polarized neutron experiments.

Single crystals of  $\text{La}_2\text{CuO}_{4+x}$  grown from  $\text{CuO}$  flux were used for these studies. The crystal orientation, lattice parameters and mosaicity (less than  $0.05^\circ$  along the  $\hat{c}$ -axis) were determined by X-ray diffractometry. Surplus oxygen was removed by annealing in vacuum. The lattice parameters correspond to the low-temperature orthorhombic stoichiometric  $\text{La}_2\text{CuO}_4$  ( $Bmab$  space group) [19]. The Néel temperature  $T_N = 320$  K was measured by SQUID.

Time-differential  $\mu\text{SR}$  experiments using 100% spin-polarized positive muons were carried out on the M15 surface muon channel at TRIUMF using the *HiTime* spectrometer. At low temperature, the zero-field (ZF)  $\mu\text{SR}$  spectra consist of two components (small and large amplitude), well known from previous studies and indicative of two inequivalent muon sites in AFM  $\text{La}_2\text{CuO}_4$ . The Néel temperature and magnetic fields at the muon sites  $B_\mu = 428.7$  G (high-frequency, large amplitude component) and  $B_\mu = 111.8$  G (low-frequency, small amplitude component) [20] are consistent with earlier studies.

In high magnetic field  $H$  applied transverse to the muon spin polarization and parallel to the  $\hat{c}$ -axis of the  $\text{La}_2\text{CuO}_4$  crystal,  $\mu\text{SR}$  spectra exhibit at least 7 signal components (Fig. 1). The central line at about 135.6 MHz coincides with the single line detected in  $\text{CaCO}_3$ , a non-magnetic reference sample, and originates from muons that miss the sample and stop in a non-magnetic environment. Two small peaks positioned around the central line correspond to the AFM splitting of the low-frequency (low-amplitude) signal observed in zero magnetic field. Our main interest is focused on the large-amplitude signals positioned symmetrically around the central line. We associate these signals with the high-frequency (large-amplitude) signal in zero magnetic field. The evolution of  $\mu\text{SR}$  spectra with temperature is presented in Fig. 2.

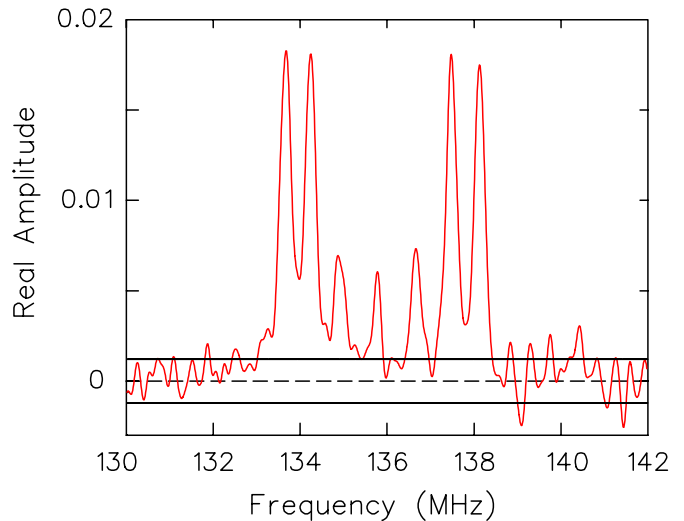


FIG. 1: Frequency spectrum of muon spin precession in AFM stoichiometric  $\text{La}_2\text{CuO}_4$  in a transverse magnetic field of  $H = 1$  T at  $T = 100$  K. The central line frequency coincides with that detected in a  $\text{CaCO}_3$  reference sample.

Within the AFM phase, one should expect 4 distinct signals in the high-field  $\mu\text{SR}$  spectra from two independent (and distinct) muon sites in the AFM host. Instead, we detect at least 6 peaks coming from muons stopped in the  $\text{La}_2\text{CuO}_4$  crystal. This may indicate that, apart from the AFM fields, there is *an additional source of magnetic field on the muon* which causes the characteristic splitting of the large-amplitude signals (see Figs. 1 and 2). To determine the origin of this field, one needs a detailed interpretation of the  $\mu\text{SR}$  spectra based on the muon sites in  $\text{La}_2\text{CuO}_4$ .

Identification of the muon stopping sites from ZF- $\mu\text{SR}$

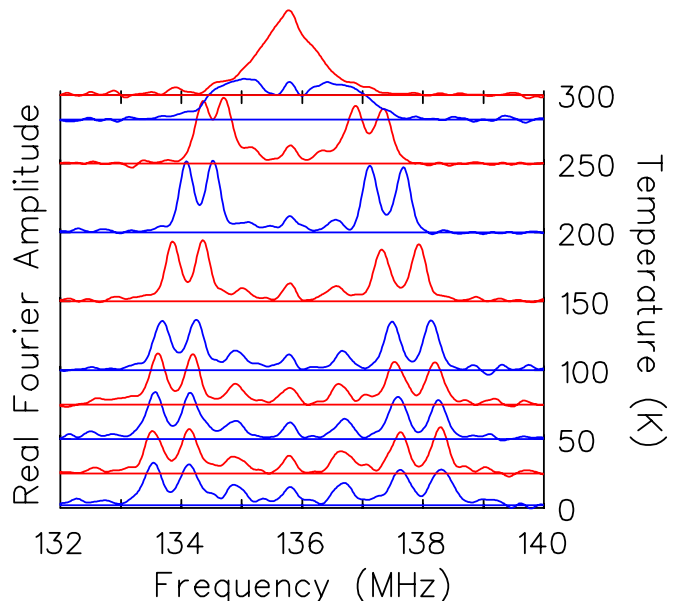


FIG. 2: Fourier transforms of the muon spin precession signal in AFM stoichiometric  $\text{La}_2\text{CuO}_4$  in an external magnetic field of  $H = 1$  T at different temperatures. Again, the central line corresponds to the background signal.

spectra has been discussed by many authors [21–25]. However, information obtained from ZF spectra alone is insufficient and additional guidance is typically sought from first-principles electronic structure calculations. It is common to predict the muon stopping site to be in the vicinity of the apical oxygen atom, but the muon positions that are actually determined are quite different in a number of studies, which leads to much confusion. In contrast, high-field  $\mu$ SR measurements, which determine the magnitudes of the *projections* (onto the directions of the applied field) of the local magnetic field at the muon, provide more precise information on the muon positions in  $\text{La}_2\text{CuO}_4$  (in combination with ZF data and the known crystal and magnetic structure of the system).

At high temperature, the  $\text{La}_2\text{CuO}_4$  crystal is tetragonal ( $I4/mmm$  space group) [26, 27] with a unit cell formed by 2 formula units. A transition to the orthorhombic phase ( $Bmab$  space group) occurs at 530 K which doubles the unit cell. This structural transition is due to rotation of the central  $\text{CuO}_6$  octahedra around the tetragonal axes (110) and antiphase rotations of octahedra in the neighbouring unit cells. At low temperature, the tilting of  $\text{CuO}_6$  octahedra reaches  $5^\circ$  [26]. Stoichiometric  $\text{La}_2\text{CuO}_4$  is a collinear AFM with four sublattices. The magnetic moment of a Cu atom amounts to  $0.66 \pm 0.13 \mu_B$  and is directed along the diagonal of the  $\text{CuO}_2$  plaquette [26, 28]. A peculiar feature of magnetic ordering in  $\text{La}_2\text{CuO}_4$  is the presence of a weak ( $\sim 0.002 \mu_B$  per Cu atom) ferromagnetic coupling of spins within  $\text{CuO}_2$  layers [26, 29] possibly originating from Dzyaloshinskii-Moriya exchange interactions and leading to a small tilting ( $\sim 0.17^\circ$ ) of Cu magnetic moments [27, 29]. These small moments are orthogonal to  $\text{CuO}_2$  layers and have opposite directions in the neighbouring planes. Thus  $\text{La}_2\text{CuO}_4$  is an antiferromagnet with hidden, weak ferromagnetism.

We determine the muon stopping sites using the dipole-field approximation and assuming the periodic AFM structure of  $\text{La}_2\text{CuO}_4$  with the known moments on Cu atoms. High-field  $\mu$ SR spectra were recorded for three different mutually orthogonal orientations of the sample, providing absolute values of the local magnetic field projections at the muon sites. There are two sites: the small-amplitude, small-field site gives the inner two peaks in TF (one for each direction of the AFM dipolar field); the large-amplitude, large-field site gives the outer peaks (each split by some additional contribution). Fig. 3 shows chemically possible muon positions consistent with the  $\mu$ SR data. The picture is quite simple: the muon is bound to an apical oxygen atom, but it can be located on the side closer to a Cu atom (large amplitude signal with higher ZF frequency) or the other side, closer to a La atom (small amplitude signal with lower ZF frequency).

The muon is located somewhat closer to the oxygen atom than expected from the typical O-H bond distance of  $\sim 1 \text{ \AA}$ . This can be explained by a small perturba-

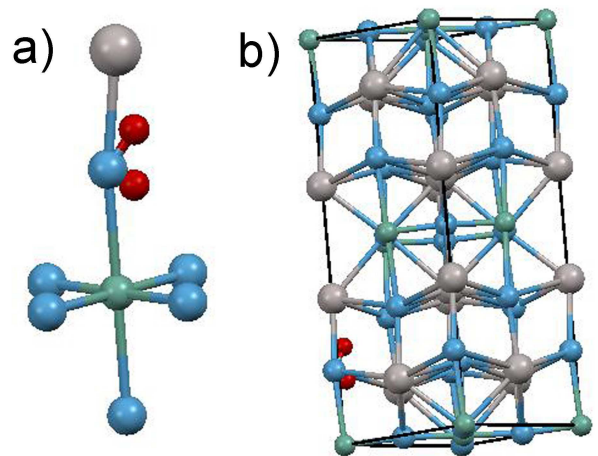


FIG. 3: Muon stopping sites as determined from dipole-field calculations and shown a) with respect to  $\text{CuO}_6$  octahedra, b) within  $Bmab$  unit cell of  $\text{La}_2\text{CuO}_4$  (green - Cu atoms, grey - La atoms, blue - O atoms, red - muon positions).

tion of the loosely bound apical oxygen position due to its bonding with the muon. Other corrections (*e.g.* uncertainty in the value of the magnetic moment on Cu and approximations of the computational procedure) are estimated to be small and therefore insignificant to the general conclusions.

The magnetic fields are almost indifferent to the tilting of  $\text{CuO}_6$  octahedra because the canted component of the moment on Cu is very small. Nevertheless, the tilting produces two types of structurally inequivalent positions for muons differing in the distance between the muon and the apical oxygen atom: shortened (SD) and elongated (ED) (Fig. 3 shows ED muon positions). The ED position seems preferable, as it produces less perturbations on oxygen. In any case, the choice between ED and SD does not affect our conclusions.

The observed splittings cannot be explained by different muon sites: In high magnetic field applied along the  $\hat{c}$ -axis, a spin-flop transition to weak ferromagnetism takes place [27, 29]. The direction of small ferromagnetic moments in every  $\text{CuO}_2$  plane becomes the same and is accompanied by reversal of in-plane components of magnetic moments for every second  $\text{CuO}_2$  plane. At  $T = 250 \text{ K}$ , SQUID measurements of our samples show that a spin-flop transition occurs in a magnetic field  $H \sim 4 \text{ T}$  [20]. The jump of magnetization  $\sim 0.002 \mu_B$  is consistent with the literature data [27, 29]. Such a transition makes the magnetic unit cell equivalent to the crystallographic unit cell and the number of magnetic sublattices decreases from four to two. This spin-flop transition is clearly seen in  $\mu$ SR measurements at 250 K (see Fig. 4) where half of the lines in the spectra vanish in a magnetic field of about 4 T. A similar feature does not show up in  $\mu$ SR spectra at 50 K as the critical field of spin-flop transition depends strongly on the temperature and the doping level of  $\text{La}_2\text{CuO}_4$ : A sample with

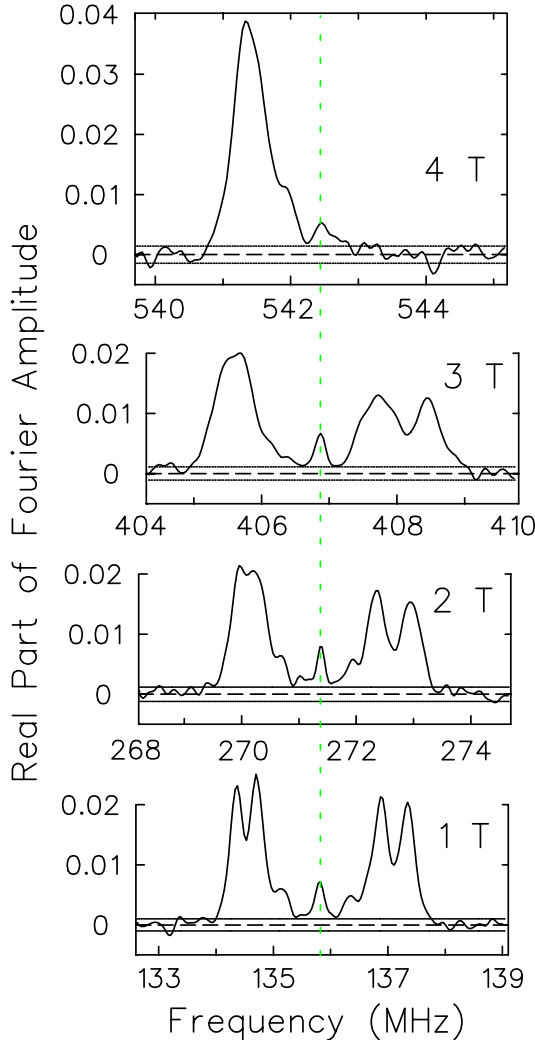


FIG. 4: Fourier transforms of the muon spin precession signals in AFM stoichiometric  $\text{La}_2\text{CuO}_4$  at  $T = 250$  K in different external magnetic fields directed along the  $\hat{c}$ -axis of the crystal. The central line corresponds to the background signal.

$T_N \sim 234$  K has  $H_c \sim 3$  T at 200 K [29] while a sample with  $T_N \sim 316$  K has  $H_c \sim 12$  T at 1.8 K [30]. The changes in the spectra verify that *muons occupy only half of the possible crystallographic positions* (either ED or SD).

Since the splitting of the large amplitude lines cannot be explained by the inequivalence of crystallographic positions brought on by tilting of the  $\text{CuO}_6$  octahedra, one can try to ascribe it to structural deformations leading to two types of tilted octahedra. Indeed, there are suggestions that a lower symmetry ( $Bm11$  space group) is possible for  $\text{La}_2\text{CuO}_4$ , but our calculations show that the proposed structural deformations are more than 3 times smaller than the difference in muon positions required to explain such a large splitting of the lines. Moreover, equal amplitudes of the split signals (see Fig. 1) would be a surprising coincidence for different muon stopping sites.

Therefore we conclude that the splittings are due to an

additional source of the magnetic field (besides AFM). This field can not originate from the apical oxygens because it should cause comparable splittings of both low- and high-frequency signals. Instead, the source of this additional magnetic field is likely confined within  $\text{CuO}_2$  planes. Then the apparent absence of splittings in the low-frequency signals can be easily explained by the increased distance from the muon to  $\text{CuO}_2$  planes, leading to much smaller splittings that are not resolved in the experiment.

There are two major types of models explaining intra-unit-cell magnetic order in cuprates. One is based on spin polarization of oxygen atoms while the other relies upon circulating orbital currents. Polarized neutron experiments have not been able to differentiate the existing models beyond establishing TRSB [10, 11]. In contrast, high-field  $\mu\text{SR}$  experiments (in combination with simple symmetry considerations) may provide such differentiation as the ratio of splittings for different directions of the magnetic field differs for different models.

The first class of models is based on the AFM ordering of spins on in-plane oxygen atoms (see Fig. 5a). When the spins are directed along the  $\hat{a}$ -axis [10] the model has the correct symmetry structure to describe the splittings in the  $\mu\text{SR}$  spectra, but the ratio of splittings along the  $\hat{b}$ - and  $\hat{c}$ -axes is about 1.6, while our experiments determine it to be close to 1.0. More importantly, this model predicts large ( $\sim 40$  G) splitting of the high-frequency signal in the absence of magnetic fields, which is not observed in the ZF- $\mu\text{SR}$  spectra. An alternative model with antiferromagnetic ordering of spins directed along the  $\hat{c}$ -axis [31] has an incorrect symmetry structure since it does not provide splitting of signals for fields along the  $\hat{c}$ -axis.

Alternatively, magnetic order can be based on current loops within the unit cell. The original model  $CC-\Theta_I$  (Fig. 5b) is formed by 4 orbital current loops O-Cu-O for each  $\text{CuO}_2$  plaquette [6]. This model is not consistent with either polarized neutron experiments or our  $\mu\text{SR}$  data, as the symmetry of the model prevents the splitting of signals for fields directed along the  $\hat{c}$ -axis. An alternative one-band model with staggered orbital current phase formed by Cu-Cu-Cu currents [32] (Fig. 5c) has correct symmetry properties but the calculated ratio of splittings along the  $\hat{b}$ - and  $\hat{c}$ -axes is too large and the absence of splitting in the ZF spectra can not be explained within this model.

The most widely used CC model of intra-unit-cell magnetic order is  $CC-\Theta_{II}$  (Fig. 5d) with two opposite current loops O-Cu-O per  $\text{CuO}_2$  plaquette [7]. The basic symmetry properties are correct and the calculated ratio of splittings along the  $\hat{b}$ - and  $\hat{c}$ -axes ( $\sim 1.1$ ) is close to the experimental value, provided that the moments follow the natural tilting of  $\text{CuO}_6$  octahedra and the muon occupies ED positions. However, this model still provides an incorrect description of ZF- $\mu\text{SR}$  spectra.

Polarized neutron experiments reveal that for differ-



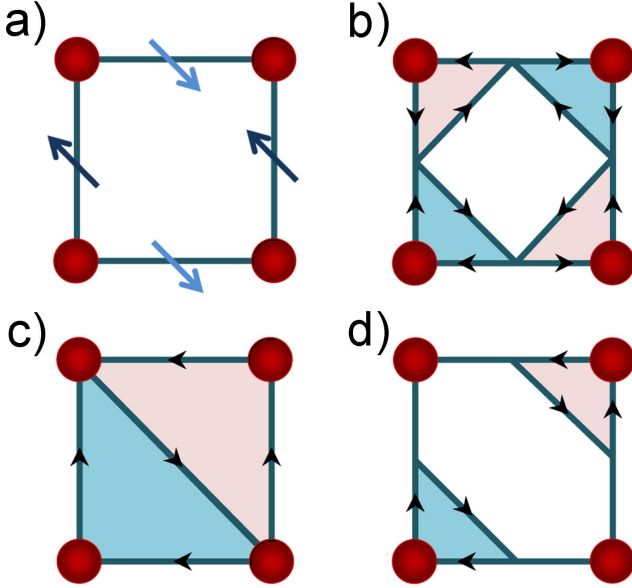


FIG. 5: Proposed sources of magnetic order in  $\text{La}_2\text{CuO}_4$ : a) AFM order of spins on oxygen atoms; b)  $CC-\Theta_I$  model with 4 orbital current loops per  $\text{CuO}_2$  plaquette; c) staggered orbital current phase with Cu-Cu-Cu current loops; d)  $CC-\Theta_{II}$  model with two opposite current loops O-Cu-O per plaquette.

ent families of cuprates the moments responsible for the intra-unit-cell magnetic order should be significantly tilted, with a tilting angle  $45 \pm 20^\circ$  [10, 11]. This constitutes a significant departure from the original CC model predicting the orbital moments to be orthogonal to  $\text{CuO}_2$  planes. However, attempts to reconcile the theory and the experiment have been made based on accounts of spin-orbit interactions [33] and quantum interference of current loop states [34]. Our calculations show that the correct ratio of splittings is achieved for a tilting of orbital moments by  $\sim 53^\circ$  within the  $CC-\Theta_{II}$  model. Moreover, this modified model is the only one consistent with zero magnetic field data: the changes of the magnetic field have opposite signs for the in-plane component and that along the  $\hat{c}$ -axis; thus the splitting of the ZF signal becomes small and hence not resolved in ZF- $\mu\text{SR}$  experiments. The orbital moment extracted from our data amounts to about  $0.04 \mu_B$ , which is comparable with the theoretical value on the order of  $0.1 \mu_B$  [6].

One puzzling characteristic of the spectra must be mentioned. In high magnetic field parallel to the  $\hat{c}$ -axis, the splitting of the component antiparallel to the field decreases while the splitting of the component parallel to the field increases; the spin-flop transition decreases the splitting. This effect is not detected with magnetic fields applied along the other axes. This peculiarity can be phenomenologically described if one assumes modula-

tion of the tilting angle for the orbital magnetic moments due to their coupling to the canting of moments on Cu. However, we see no apparent reason for such coupling, which calls for additional studies.

In summary, high magnetic field  $\mu\text{SR}$  studies in orthorhombic  $\text{La}_2\text{CuO}_4$  reveal an additional source of magnetic field within the unit cell, consistent with the Varma model of circulating currents in cuprates.

This work was supported by Kurchatov Institute, NSERC of Canada and the U.S. DOE, Basic Energy Sciences (Grant de-sc0001769).

---

\* Electronic address: mussr@triumf.ca

- [1] M. R. Norman and C. Pépin, Rep. Prog. Phys. **66**, 1547 (2003).
- [2] J. L. Tallon and J. W. Loram, Physica C **349**, 53 (2001).
- [3] T. Timusk and B. Statt, Rep. Prog. Phys. **62**, 61 (1999).
- [4] A. Kaminski *et al.*, Nature **416**, 610 (2002).
- [5] V. J. Emery and S. A. Kivelson, Nature **374**, 434 (1995).
- [6] C. M. Varma, Phys. Rev. B **55**, 14554 (1997).
- [7] C. M. Varma, Phys. Rev. B **73**, 155113 (2006).
- [8] S. Chakravarty *et al.*, Phys. Rev. B **63**, 094503 (2001).
- [9] S. N. Borisenko *et al.*, Phys. Rev. Lett. **92**, 207001 (2004).
- [10] B. Fauqué *et al.*, Phys. Rev. Lett. **96**, 197001 (2006).
- [11] H. A. Mook *et al.*, Phys. Rev. B **78**, 020506 (2008).
- [12] Y. Li *et al.*, Nature **455**, 372 (2008).
- [13] J. H. Brewer, in *Encyclopedia of Applied Physics*, Vol. 11 (VCH Publishers, New York, 1994); A. Yaouanc and P. Dalmas de Reotier, *Muon Spin Rotation, Relaxation, and Resonance* (Oxford University Press, 2011).
- [14] J. E. Sonier *et al.*, Science **292**, 1692 (2001).
- [15] J. E. Sonier *et al.*, Phys. Rev. B **66**, 134501 (2002).
- [16] G. J. MacDougall *et al.*, Phys. Rev. Lett. **101**, 017001 (2008).
- [17] A. Shekhter *et al.*, Phys. Rev. Lett. **101**, 227004 (2008).
- [18] C. Weber *et al.*, Phys. Rev. Lett. **112**, 117001 (2014).
- [19] O. E. Parfenov *et al.*, JETP Letters **76**, 616 (2002).
- [20] V. G. Storchak *et al.*, to be published.
- [21] B. Hitti *et al.*, Hyperf. Int. **63** 287, (1990).
- [22] S. B. Sulaiman *et al.*, Phys. Rev. B **49**, 9879 (1994).
- [23] H. U. Suter *et al.*, Physica B **326**, 329 (2003).
- [24] W. Huang *et al.*, Phys. Rev. B **85**, 104527 (2012).
- [25] B. Adiperdana *et al.*, AIP Conf. Proc. **1554**, 214 (2013).
- [26] D. C. Johnston, J. Magn. Magn. Mat. **100**, 218 (1991).
- [27] M. A. Kastner *et al.*, Rev. Mod. Phys. **70**, 897 (1998).
- [28] O. Schärpf and H. Capellmann, Z. Phys. B: Cond. Matt. **80**, 253 (1990).
- [29] T. Thio *et al.*, Phys. Rev. B **38**, 905 (1988).
- [30] M. Reehuis *et al.*, Phys. Rev. B **73**, 144513 (2006).
- [31] A. S. Moskvina, JETP Letters **96**, 385 (2012).
- [32] T. D. Stanescu and P. Phillips, Phys. Rev. B **69**, 245104 (2004).
- [33] V. Aji and C. M. Varma, Phys. Rev. B **75**, 224511 (2007).
- [34] Y. He and C. M. Varma, Phys. Rev. Lett. **106**, 147001 (2011).